Supporting Information

Hairpin probe-mediated Exponential Amplification

Reaction for Highly Sensitive and Specific Detection of

microRNAs

Hongyan Yu[a, 1], Zhi Weng[a, 1], Xi Zhou[a], Dan Bai [a], Wang Luo[a], Xiaole Han

[a], Lin Song [a], Qian Liu [a], Junjie Li[a], Yujun Yang[a], Yongcan Guo [c,]*, Ke Lv

[b,]*, Guoming Xie [a,]*

a   *Key Laboratory of Clinical Laboratory Diagnostics (Chinese Ministry of*

Education), College of Laboratory Medicine, Chongqing Medical Laboratory

Microfluidics and SPRi Engineering Research Center, Chongqing Medical

University, No. 1 Yi Xue Yuan Road, Chongqing 400016, P.R China.

b   *Department of Neurosurgery, The First Affiliated Hospital of Chongqing Medical*

University, No.1 Youyi Road, Chongqing 40016, P.R China.

c   *Clinical Laboratory of Traditional Chinese Medicine Hospital Affiliated to*

Southwest Medical University, LuZhou Key Laboratory of Nanobiosensing and

Microfluidic Point-of-Care Testing, Luzhou 646000, P.R China.

Corresponding author:

Guoming Xie, Key Laboratory of Clinical Laboratory Diagnostics (Chinese Ministry of

Education), College of Laboratory Medicine, Chongqing Medical Laboratory

Microfluidics and SPRi Engineering Research Center, Chongqing Medical University,

No. 1 Yi Xue Yuan Road, Chongqing 400016, P.R China.

E-mail address: guomingxie@cqmu.edu.cn, xiegm059@foxmail.com

Tel.: +86 23 68485240; Fax.: +86 23 68485239

Ke Lv, Department of Neurosurgery, The First Affiliated Hospital of Chongqing

Medical University, No.1 Youyi Road, Chongqing 40016, P.R China.

E-mail: sxccq2021@163.com

Yongcan Guo, Luzhou Key Laboratory of Nanobiosensing and Microfluidic Point-of-

28 *Care Testing, Clinical Laboratory of Traditional Chinese Medicine Hospital Affiliated*

29 *to Southwest Medical University, Luzhou 646000, P.R China.*

30 *E-mail: swtcmlab@163.com*

31 Hongyan Yu, and Zhi Weng contributed equally to this work.

32

Materials and reagents

All the oligonucleotides used in this work were synthesized by Sangon Biotech Inc. (Shanghai, China) with HPLC purification (corresponding sequences are listed in Table S1). Bst DNA Polymerase (Large Fragment), Nt.BsmAI, CutSmart buffer (20 mM Tris-acetate, 50 mM potassium acetate, 10 mM magnesium acetate and 100 mg/ml BSA, pH 7.9) were ordered from New England Biolabs (New England, USA). Deoxynucleotide triphosphates (dNTPs), SYBR Green, diethylpyrocarbonate (DEPC)-treated water, 8 strip real-time PCR tubes and TBE solution were purchased from Sangon Biotech Inc. (Shanghai, China). DNA loading buffer (6×) and Gel Red nucleic acid dye were ordered from TaKaRa Biotech (Dalian, China). The human serum was obtained from the First Affiliated Hospital of Chongqing Medical University.

Apparatus and instruments

Gel images were obtained on electrophoresis apparatus (DYY-6C, LIUYI, China) and imaging system (Bio-Rad Laboratories, USA). PCR assay was conducted by real-time PCR instrument (CFX96, Bio-Rad, USA). All chemical reagents were of analytical grade, and RNase-free water was used throughout this study.

Experimental section

PAGE analysis of HEAR

The reaction solution (20μL) was prepared separately as a part A solution and part B solution. The part A solution consisted of miRNA (10 nM), H1 (200 nM), and H2 (200 nM). The part B solution consisted of dNTP (250 μM), Bst DNA Polymerase (1.6 U), Nt.BsmAI nicking endonuclease (5 U), CutSmart buffer (1×), SYBR I (2×), and RNase-free. At first, the part A solution was incubated at room temperature for 5 minutes. Subsequently, part A and part B were mixed, the polymerization reaction was performed at 43 °C for 15 min.

Products of reactions were analyzed by running in a 12% native polyacrylamide gel. Electrophoresis was performed in 1× TBE buffer (2 mM EDTA and 89 mM Tris-boric acid, pH 8.3) at a 100 V constant voltage for 60 min before staining with 4S GelRed. Finally, the gel was visualized via a gel image system.

Real-time Fluorescence Measurement of HEAR and PEAR.

63   To detect different concentrations of miRNA, the part A solution consisted of H1

64 or P1 (200 nM), and H2 (200 nM). The part B solution consisted of dNTP (250 μM),

65 Bst DNA Polymerase (1.6 U), Nt.BsmAI nicking endonuclease (5 U), CutSmart buffer

66 (1×), SYBR I (2×), and RNase-free. Firstly, the part A solution was incubated at room

67 temperature for 5 minutes. Subsequently, part A and part B were mixed at 43 °C, and

68 the fluorescence intensity was monitored at intervals of 30 seconds by a CFX96™ Real-

69 Time PCR Detection System with the SYBR filter set.

70

71 **Table S1.** Sequences of the designed oligonucleotides.

Oligonucleotides	Sequence (from 5′ to 3′)
let7a	UGAGGUAGUAGGUUGUAUAGUU
let7b	UGAGGUAGUAGGUUGUGUGGUU
let7c	UGAGGUAGUAGGUUGUAUGGUU
let7d	AGAGGUAGUAGGUUGCAUAGUU
let7e	UGAGGUAGGAGGUUGUAUAGUU
let7f	UGAGGUAGUAGAUUGUAUAGUU
let7g	UGAGGUAGUAGUUUGUACAGUU
let7i	UGAGGUAGUAGUUUGUGCUGUU
Primer of PEAR:	
P1	CGGA<u>GTCTCT</u>↓AACTATACAACCAAAA-p
P2	CGGA<u>GTCTCT</u>↓TGAGGTAGTAGGAAAA-p
Hairpin of HEAR:	
H1(6bp stem)	TATAGTT<u>GTCTCT</u>↓AACTATACAACCAAAA-p
H2(6bp stem)	ACCTCA<u>GTCTCT</u>↓TGAGGTAGTAGGAAAA-p
H3(6+1bp stem)	ATAGTTG<u>GTCTCT</u>↓CAACTATACAACCAAAA-p
H4(6+1bp stem)	ACCTCAG<u>GTCTCT</u>↓CTGAGGTAGTAGGAAAA-p
H5(6+2bp stem)	ATAGTTG<u>GTCTCT</u>↓CAAACTATACAACCAAAA-p
H6(6+2bp stem)	ACCTCATG<u>GTCTCT</u>↓CATGAGGTAGTAGGAAAA-p
H5(6+3bp stem)	ATAGTTGTG<u>GTCTCT</u>↓CACAACTATACAACCAAAA-p
H6(6+3bp stem)	ACCTCAGTG<u>GTCTCT</u>↓CACTGAGGTAGTAGGAAAA-p

72   Note:

73   [a] The sequence underlined is the recognition site of the nicking enzyme Nt.BsmAI.

74   [b] "↓" represents the cleavage site.

75   [c] The 'p' indicates as phosphate group.

76

77   **Table S2** Comparison of analytical performance for miRNA detection methods.

Method	Analytes	One-step reaction	Linear range	Detection limit	Reference
Fluorescent assay	miR-141	Yes	100 pM-100 nM	100 fM	[1]
Fluorescent assay	miR-21	Yes	10 fM-1 nM	10 fM	[2]
Fluorescent assay	miR-21	Yes	1 fM-100 pM	100 aM	[3]
Fluorescent assay	miR-21	no	10 fM-10 pM, 10 pM-100 nM	10 fM	[4]
Fluorescent assay	miR-21	no	100 aM-100 pM	70 aM	[5]
Fluorescent assay	miR-21	/	150 pM-37.5 nM	130 pM	[6]
Fluorescent assay	Let7a	no	100 aM-10 nM	84.5 aM	[7]
Fluorescent and visual assay	Let7a	no	100 aM -10 pM	100 aM	[8]
TIRFM	Let7a	no	0−25 pM	500 fM	[9]
Electrochemical assay	miR-21	no	1 pM-10 nM	260 fM	[10]
Electrochemiluminescence assay	miR-21	no	1 fM-100 pM	650 aM	[11]
Electrochemiluminescence assay	miR-21	no	10 fM-100 pM	6.6 fM	[12]
Surface-enhanced Raman spectroscopy	miR-21	no	1 fM-100 pM	393 aM	[13]
Fluorescent assay	Let7a	yes	100 aM-10 nM	19 aM	This work

78

79

80

81

82 **Supplementary Figures**
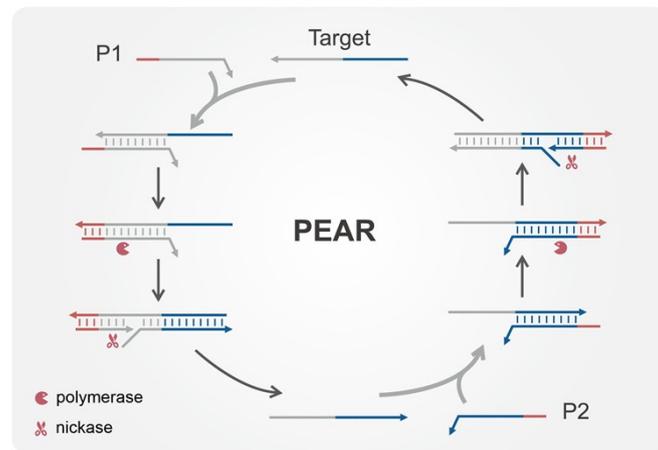
83 **Figure S1.** Schematic illustration of primer probe-mediated exponential amplification

84 reaction (PEAR)

85

A — MFE structure at 43.0 C

Free energy of secondary structure: -3.50 kcal/mol

B — MFE structure at 43.0 C

Free energy of secondary structure: -3.50 kcal/mol
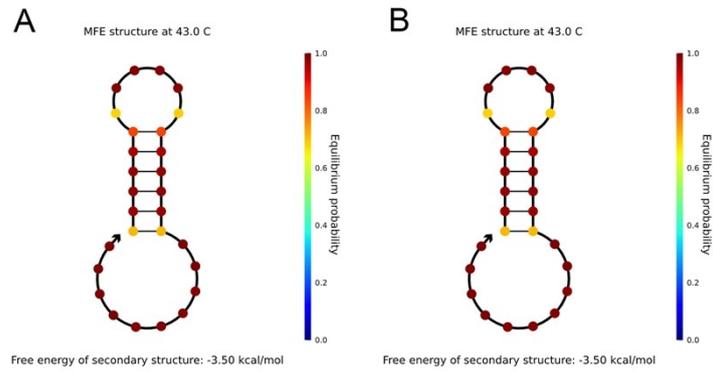
86 **Figure S2.** Minimum free energy (MFE) structure of (A) H1 and (B) H2 at 43 °C. The

87 MFE structures were analyzed by NUPACK web server (http://www.nupack.org/).

88
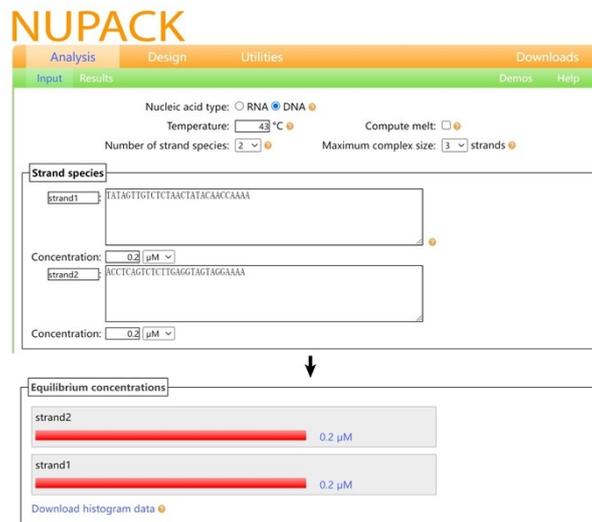
89 **Figure S3.** Simulation of hybridization between H1 and H2 through NUPACK

90 software (http://www.nupack.org/).

91

92 The reaction temperature is essential to the strand displacement reaction and enzyme

93 activity. As illustrated in Fig. S4, although the difference between positive and negative

94 signals were similar at different temperatures, the fastest reaction efficiency was seen

95 at 43°C. Therefore, 43°C was selected as the reaction temperature in the following

96 study.
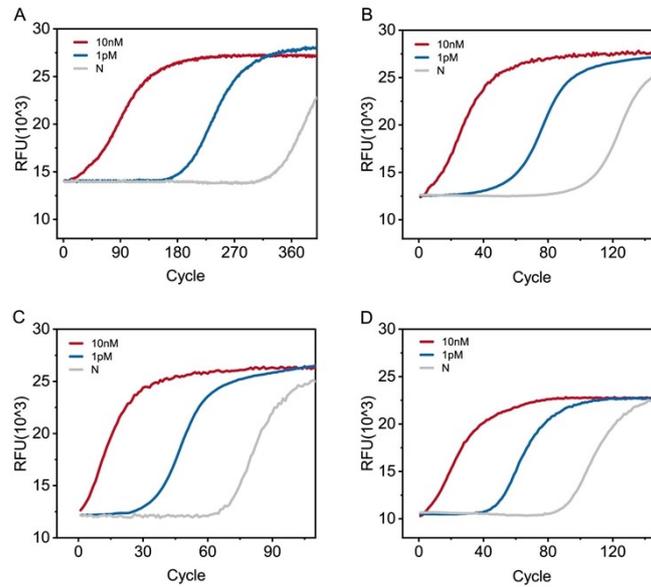
97 **Figure S4.** The effect of temperature on HEAR. Real-time fluorescence quantitative

98 curves were generated at (A) 30°C (B) 37°C (C) 43°C and (D) 50°C, respectively.

99

The enzyme concentration directly affects speed of the enzyme-based isothermal amplification reactions and the generation of non-specific signals to a large extent. Although the precise mechanism of the interaction between nicking endonuclease and polymerase is not well understood, it is possible to simply modulate the reaction by changing the concentration of the enzymes. When the concentration of the immobilized polymerase was 1.6 U, the real-time fluorescence curves of 10 U, 5 U, 2.5 U and 1.25 U nicking endonuclease concentrations were measured respectively (Fig. S5). At the same time, when the concentration of nicking endonuclease was fixed at 5 U, the real-time fluorescence curves of 3.2 U, 1.6 U, 0.8 U and 0.4 U polymerase were measured respectively (Fig. S6). It can be seen from Fig. S5-6 that the reaction speed became faster with the increase of enzyme concentration, and the POI difference between negative and positive signals was similar, indicating that the strand displacement reaction and the design of poly(A) effectively hindered the generation of non-specific signals. We next performed real-time fluorescence quantitative detection of different concentrations of miRNA under high concentrations of polymerase (3.2 U polymerase, 5 U nicking endonuclease), and plotted the correlation linear curve (Fig. S7). Considering the reaction performance and cost, 5U nicking endonuclease and 1.6U polymerase were selected for the following experiments.
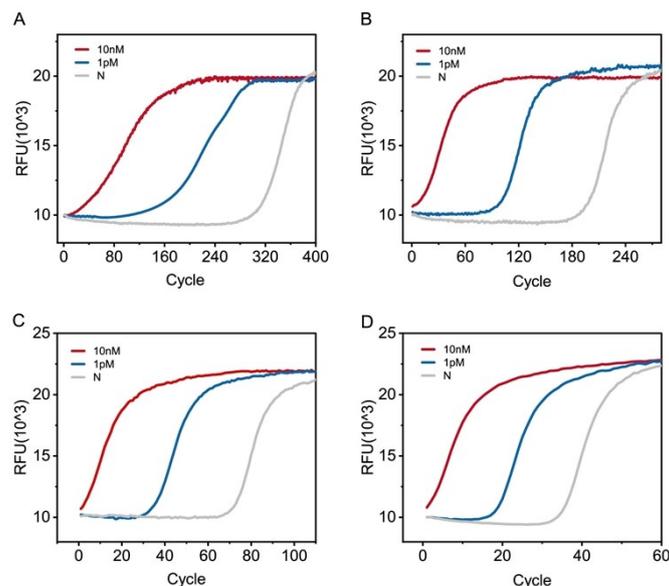
118 **Figure S5.** The effect of nicking endonuclease concentrations on HEAR. Real-time

119 fluorescence quantitative curves were generated at (A) 1.25 U (B) 2.5 U (C) 5 U and

120 (D) 10 U, respectively.
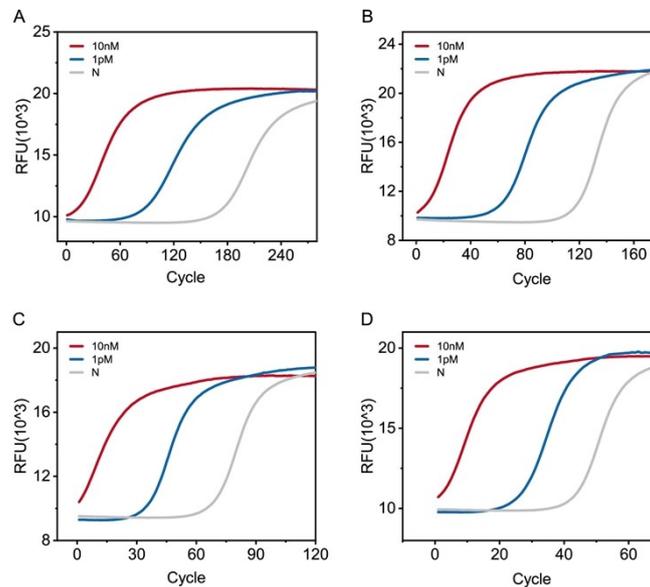
121 **Figure S6.** The effect of polymerase concentrations on HEAR. Real-time fluorescence

122 quantitative curves were generated at (A) 0.4 U (B) 0.8 U (C) 1.6 U and (D) 3.2 U,

123 respectively.

124
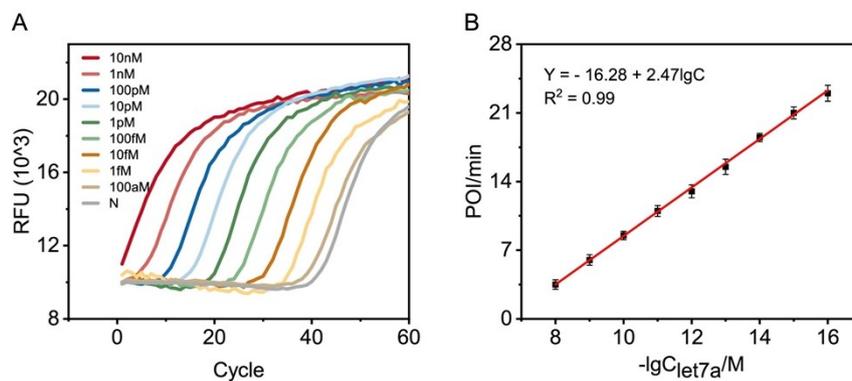
125 **Figure S7.** (A) Real-time fluorescence quantitative curve of HEAR triggered by

126 different miRNAs at high concentrations of polymerase (3.2U). (B) Linear relationship

127 between POI of HEAR and logarithm of miRNA concentration.

128

129

131 In general, when the Gibbs free energy change of the reaction approaches 0 kcal/mol,
132 such as branch migration reactions, even a single base mismatch that causes a small
133 thermodynamic change can cause enough thermodynamic difference and reduce the
134 yield compared to matching target.31 Therefore, we wondered whether increasing the
135 stem length of the hairpin could achieve increased specificity of HEAR. 1, 2 and 3
136 base pairs were added between stem and loop for testing. As shown in Fig. S8, as the
137 number of bases increased, the amplification efficiency became lower. We speculated
138 that it may be due to the difficulty in opening the hairpin after adding bases, and the
139 low yield caused by its reversibility. Therefore, we still chose not to add additional
140 base pairs between the loop and the stem.
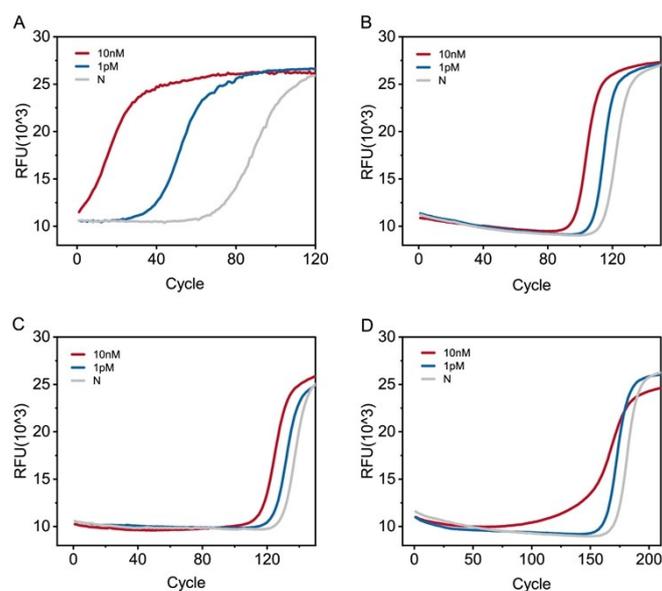
141 **Figure S8.** Effects of hairpin stem length on HEAR. (A) Real-time fluorescence
142 quantitative curves triggered by hairpins for 6nt (B) 6+1bp (C) 6+2bp and (D) 6+3bp
143 stem lengths.

144
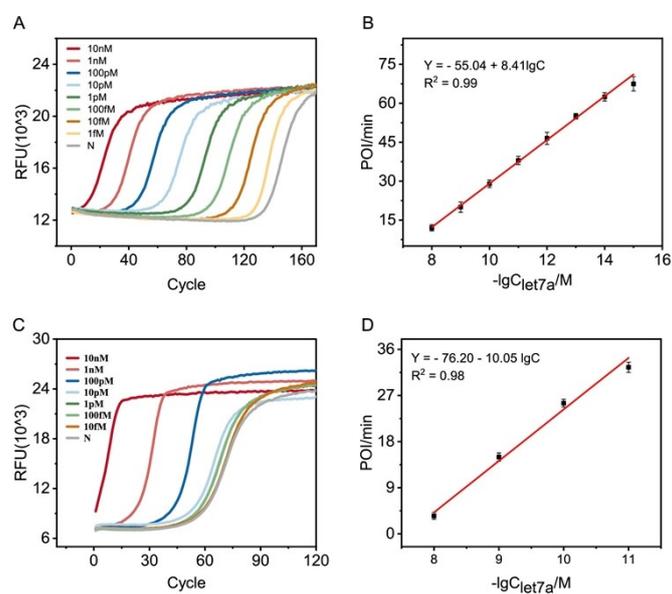
145 **Figure S9.** (A) Real-time fluorescence quantitative curve of HEAR triggered by

146 different miRNAs at 37°C. (B) Linear relationship between POI of HEAR and

147 logarithm of miRNA concentration. (C) Real-time fluorescence quantitative curve of

148 PEAR triggered by different miRNAs at 37°C. (D) Linear relationship between POI of

149 PEAR and logarithm of miRNA concentration.

Reference:

1. B. C. Yin, Y. Q. Liu and B. C. Ye, *J. Am. Chem. Soc.*, 2012, **134**, 5064-5067.
2. R. Duan, X. Zuo, S. Wang, X. Quan, D. Chen, Z. Chen, L. Jiang, C. Fan and F. Xia, *J. Am. Chem. Soc.*, 2013, **135**, 4604-4607.
3. C. Yuan, J. Fang, X. Luo, Y. Zhang, G. Huang, X. Zeng, K. Xia, M. Li, X. Chen, X. Yang, M. L. de la Chapelle and W. Fu, *Anal. Chim. Acta.*, 2022, **1203**, 339706.
4. X. Chen, Y. Deng, G. Cao, Y. Xiong, D. Huo and C. Hou, *Chem. Commun. (Camb)*, 2021, **57**, 6129-6132.
5. S. Peng, Z. Tan, S. Chen, C. Lei and Z. Nie, *Chem. Sci.*, 2020, **11**, 7362-7368.
6. J. Su, F. Wu, H. Xia, Y. Wu and S. Liu, *Chem. Sci.*, 2020, **11**, 80-86.
7. C. C. Li, J. Hu, X. Zou, X. Luo and C. Y. Zhang, *Anal. Chem.*, 2022, **94**, 1882-1889.
8. M. Zhang, H. Wang, H. Wang, F. Wang and Z. Li, *Anal. Chem.*, 2021, **93**, 7942-7948.
9. Y. Qi, Y. Zhai, W. Fan, W. Ren, Z. Li and C. Liu, *Anal. Chem.*, 2021, **93**, 1620-1626.
10. D. Zhu, W. Liu, D. Zhao, Q. Hao, J. Li, J. Huang, J. Shi, J. Chao, S. Su and L. Wang, *ACS Appl. Mater. Interfaces.*, 2017, **9**, 35597-35603.
11. Y. Xia, T. Chen, L. Zhang, X. Zhang, W. Shi, G. Chen, W. Chen, J. Lan, C. Li, W. Sun and J. Chen, *Biosens. Bioelectron.*, 2021, **173**, 112834.
12. P. Zhang, J. Jiang, R. Yuan, Y. Zhuo and Y. Chai, *J. Am. Chem. Soc.*, 2018, **140**, 9361-9364.
13. C. Y. Song, Y. J. Yang, B. Y. Yang, Y. Z. Sun, Y. P. Zhao and L. H. Wang, *Nanoscale*, 2016, **8**, 17365-17373.